OncoTargets and Therapy

Dovepress
open access to scientific and medical research

Open Access Full Text Article

ORIGINAL RESEARCH

miR-431-5p alters the epithelial-to-mesenchymal transition markers by targeting *UROC28* in hepatoma cells

This article was published in the following Dove Press journal:
OncoTargets and Therapy

Qinglei Kong[1,*]
Jianhua Han[1,*]
Hong Deng[2]
Feilong Wu[1]
Shaozhong Guo[2]
Zhiqiang Ye[1]

[1]Department of Emergency, The Third Affiliated Hospital of Sun Yat-San University, Guangzhou 510630, China; [2]Department of Infectious Disease and Clinical Laboratory, The Third Affiliated Hospital of Sun Yat-San University, Guangzhou 510630, China

*These authors contributed equally to this work

Objective: MicroRNA (miR)-431 plays an essential role in various human cancer types, particularly in the process of invasion. However, the function and mechanism of miR-431-5p in the invasion of hepatocellular carcinoma (HCC) remain undefined.

Methods: The expression levels of miR-431-5p and its potential target protein *UROC28* in hepatocellular carcinoma cells and tissues were detected, and the levels of EMT markers in vivo and in vitro were also detected.

Results: MiR-431-5p was downregulated in HCC cell lines and tissues and associated with vascular invasion and tumor encapsulation. Furthermore, miR-431-5p was able to influence the epithelialto- mesenchymal transition (EMT) process in HCCLM3 and HUH7 cells. Mechanistically, it was discovered that miR-431-5p repressed invasion by targeting *UROC28*. Furthermore, miR-431-5p influenced the EMT markers in HCCLM3 and HUH7 cells by downregulating *UROC28* expression. Similarly, in vivo assays confirmed that miR-431-5p upregulation in HCC cells remarkably inhibited tumor proliferation and influenced the EMT markers.

Conclusion: The current study has demonstrated that the miR-431-5p/*UROC28* axis acts possible influence on the EMT in HCC. Upregulation of miR-431-5p could be an original approach for inhibiting tumor invasion.

Keywords: hepatocellular carcinoma, microRNA-431, *UROC28*, PBOV1, epithelial-to-mesenchymal transition

Introduction

Hepatocellular carcinoma (HCC) is the most malignant cancer in China, particularly in the Guangdong Province.[1] Treatment of HCC is largely futile due to the occurrence of invasion in the early stage and after surgical resection.[2] However, the mechanism of invasion of HCC has been poorly clarified. The epithelial-to-mesenchymal transition (EMT) is considered a crucial step that occurs during HCC invasion.[3] Nevertheless, current understanding about the variations that stimulate the EMT process is limited.

MicroRNAs (miR) are small noncoding RNA molecules that can broadly control the expression of various genes by binding to the 3′-UTRs of target genes.[4,5] Moreover, miRs have been shown to play a crucial role in the invasion and metastasis of cancer cells, as either EMT suppressors or inducers.[6–8] miR-431 is located on chromosome 14q32.2;[9] Pan et al found that miR-431 is a possible novel marker for renal cancer, lung cancer, and melanoma, even at the primary stage of cancer.[10–13] Meng et al[14] investigated that hsa-miR-431-5p was downregulated in the serum of diffuse large B-cell lymphoma patients. Yamaguchi et al[13] found that miR-431 could contribute to chemotherapy resistance in human cancer. In addition, Trehanpati et al[15] found that miR-431 was significantly

Correspondence: Zhiqiang Ye
Department of Emergency, The Third Affiliated Hospital of Sun Yat-San University, 600 Tianhe Road, Guangzhou 510630, China
Tel +86 20 8525 3333
Email yezhiqiang_zssy@126.com

submit your manuscript | www.dovepress.com
Dovepress
http://dx.doi.org/10.2147/OTT.S173840

expressed in hepatitis E viral (HEV) infection in liver. Other studies have also explored the relationship between miR-431 and liver disease such as HCC, but whether miR-431-5p can play a part in the invasion of HCC by means of the EMT and the mechanism of how miR-431-5p reduces the EMT in HCC have not been fully explored up to now in vitro or in vivo.[10,16] miRs contribute to the occurrence and development of cancer by regulating the posttranscriptional process of particular target genes. Numerous genes have been identified to be target genes of miR-431, including ZEB1, SOCS6, tyrosine protein kinase Fyn, and Eya4.[12,16] *UROC28*, also known as PBOV1, a key promoter of prostate cancer, hepatocellular cancer, breast cancer, and bladder cancer, is also a direct target of miR-431-5p.[17–19] Previous studies have indicated that *UROC28* plays a carcinogenic role in cancer proliferation, cell cycle, and apoptosis.[20,21] Furthermore, *UROC28* may be a key factor in inducing cancer cell invasion and metastasis.[22,23] However, whether miR-431-5p affects the expression and activity of *UROC28* in HCC has not been previously clarified to our knowledge.

In the current study, it was demonstrated that miR-431-5p expression was significantly lower in HCC cell lines and tissues compared with corresponding nontumorous cells and tissues.[10] Furthermore, it was demonstrated that down-regulation of miR-431-5p was considerably associated with vascular invasion and tumor encapsulation deficiency of HCC focus.[16] Furthermore, an increase in miR-431-5p expression in HCC cell lines may inhibit cell invasion.[10,16] A further mechanistic study revealed that *UROC28* was a direct target gene of miR-431-5p.[19] As a result, miR-431-5p may contribute to the invasion of HCC via UROC28-mediated EMT process.

Materials and methods

Clinical samples and ethics statement

HCC tissue samples and corresponding adjacent nontumor tissues (ANT) were collected from 38 patients who had undergone hepatectomy for HCC from September 2010 to September 2013 in The Third Affiliated Hospital of Sun Yat-Sen University (Guangdong, China). The clinical and animal studies were approval by the Institutional Research Ethics Committees of The Third Affiliated Hospital of Sun Yat-Sen University. Written informed consent was obtained from all patients. All patient information was obtained and used in accordance with approved protocols from the institutional review boards of the participating institutions. HCC patients were histologically confirmed by experienced liver pathologists in The Third Affiliated Hospital of Sun Yat-Sen University. None of the patients had received any adjunctive therapy. Inclusion criteria were as follows: 1) patients had not received radiofrequency ablation preoperatively; 2) Child–Pugh A/B; and 3) no concurrent cancers. Exclusion criteria were as follows: 1) recurrent HCC; 2) surgery-related death within 30 days after surgery; 3) extrahepatic metastasis; and 4) incomplete follow-up data.[24,25] Preoperative diagnosis of HCC was based on either two typical imaging findings or a combination of alpha-fetoprotein (AFP) >400 ng/mL and one imaging finding (liver ultrasonic contrast [UC] or computed tomography [CT] or magnetic resonance imaging [MRI]). Clinical variables, including gender and age, were collected from pathological reports, along with pathological characteristics including liver cirrhosis (evaluated by the Ishak score), tumor size, tumor number, degree of tumor differentiation, satellite lesions, and major vascular invasion (MVI). The mean age of the 38 patients (seven females and 31 males) was 49.65±5.52 years (range, 35–67 years). All patients were regularly followed up at months 1, 3, and 6 in the first 6 months after the operation and every 3 months thereafter. Routine blood tests, AFP levels, liver function tests, HBV markers, and HBV-DNA levels, as well as liver ultrasound results, were included at each follow-up examination. Recurrent lesions were confirmed by CT or/and MRI, or by biopsy. If there was HCC recurrence, patients were evaluated in The Third Affiliated Hospital of Sun Yat-Sen University for treatment guidance based on the status of tumor and general condition of the patient. Liver transplantation, resection, ablation, transcatheter arterial chemoembolization (TACE), and palliative therapy were recommended based on the status and general condition of the recurrent tumor.

Cell lines, cell culture, and cell transfection

The immortalized human hepatic cell line L02 and the HCC cell lines HCCLM3, HUH7, Hep3B, HepG2, HLE, HLF, and SNU423 were obtained from and authenticated by Shanghai Cell Bank of Chinese Academy of Science (Shanghai, China) and maintained at 37°C and 5% CO_2 in DMEM with 10% FBS (Thermo Fisher Scientific, Waltham, MA, USA). Human umbilical vein endothelial cells (HUVECs) were purchased from Clonetics (San Diego, CA, USA) and cultured in F12K supplemented with FBS, endothelial cells' growth supplement, and heparin (Thermo Fisher Scientific). Mycoplasma infection was tested regularly using a PCR-based kit (MP0040; Sigma-Aldrich Co., St Louis, MO, USA) and excluded in all the results presented in the manuscript. Transfection was generally performed on cells grown to about 70% density.[26] To increase the intracellular expression of miR-431-5p, miR-431-5p, or *UROC28*, oligonucleotides

were designed and cloned into the plasmid vector. Cells were transiently transfected with the miR-431-5p plasmid or negative control (NC) miR plasmid (Ambion, Austin, TX, USA) according to the manufacturer's instructions. Cells stably overexpressing miR-431-5p were generated by lentiviral transfection with a vector expressing miR-431-5p or a miR-NC vector according to the manufacturer's protocol (Lenti-miR™ microRNA precursor clones; SBI System Biosciences, Palo Alto, CA, USA). Successfully transfected cells were selected for 10 days with 0.5 μg/mL of neomycin at 48 hours after infection, and transfection was confirmed by the expression of green fluorescence protein.[27] All constructs were verified by sequencing.

RNA extraction and reverse transcription-quantitative PCR (RT-qPCR) assay

Total RNA was extracted from tissue lysates or cell samples using either an miRNeasy kit (Qiagen NV, Venlo, the Netherlands) or TRI Reagent (Sigma-Aldrich Co./EMD Millipore, Billerica, MA, USA) at room temperature for 10 minutes, according to the manufacturer's protocols, followed by reverse transcription to cDNA with TaqMan® MicroRNA Reverse Transcription Kit (Thermo Fisher Scientific) or TransScript first-strand cDNA Synthesis SuperMix kit (Qiagen NV).[28,29] Relative expression levels of miR-431-5p were determined using the TaqMan® MicroRNA Assay (Thermo Fisher Scientific) protocol specific for miR-431-5p and were normalized to that of internal control U6 by using the $2^{-\Delta\Delta Cq}$ method. Relative expression levels of *UROC28* were determined using the Premix Ex Taq™ kit (Qiagen NV) with the following primers: *UROC28* forward, TTGTGGACCTGTACCACCTAA and reverse; Zonula Occludens protein-1 (ZO-1) forward, CCAGCAAAGCAATCCCCACT and reverse; E-cadherin forward, CAGGCCTTAACCCCACAACCC and reverse; fibronectin forward, TCGAAAGATCCGCAGCACAT and reverse; and N-cadherin forward, CCACCCACAGCCACT TAACCG and reverse. The relative amount of mRNA was normalized by using GAPDH.[30] Experiments were repeated three times. The thermal cycle for miR was as follows: 95°C for 2 minutes; 94°C for 16 seconds; 63°C 35 times for 36 seconds; and 59°C for 38 seconds.

Western blot assay

The protein contents of tissues or cell lysates were measured using a bicinchoninic acid kit (GE Healthcare UK Ltd, Little Chalfont, UK). A suitable amount of total protein of each sample (10–20 μg) was then separated by 10% SDS-PAGE. Following vertical electrophoretic separation, proteins were transferred to polyvinylidene fluoride (PVDF) membranes by wet transfer. Subsequently, PVDF membranes were blocked with 5% fat-free milk for 1 hour at room temperature and then incubated with rabbit anti-UROC28 antibodies, rabbit anti-ZO-1 antibodies, rabbit anti-E-cadherin antibodies, rabbit anti-fibronectin antibodies, rabbit anti-N-cadherin antibodies, and rabbit anti-GAPDH antibodies (Santa Cruz Biotechnology Inc., Dallas, TX, USA) at 4°C overnight.[31] Membranes were washed three times in tris-buffered saline with Tween-20 (TBST) and were then incubated with HRP-conjugated secondary antibody (Bio-Rad Laboratories Inc., Hercules, CA, USA) at room temperature for 1 hour. After washing again three times with TBST, exposure and development were performed using an enhanced chemiluminescence (ECL) detection kit (GE Healthcare UK Ltd) and densities were measured using the GS-900™ Calibrated Densitometer with the Image Lab 4.1 Software from Bio-Rad Laboratories Inc. All were performed in triplicate.

Immunohistochemistry (IHC)

Tissue slides were incubated with rabbit anti-UROC28 antibodies, rabbit anti-ZO-1 antibodies, rabbit anti-E-cadherin antibodies, rabbit anti-fibronectin antibodies, rabbit anti-N-cadherin antibodies, or rabbit anti-GAPDH antibodies and 3,3′-diaminobenzidine to visualize IHC labeling. Slides were counterstained lightly with crystal violet. Normal rabbit IgG was used to confirm the specificity of the IHC labeling. Protein expression levels were scored semiquantitatively on the basis of an established immunoreactivity scoring (IRS) system. Briefly, IRS covers a range of 0–12 as a product of multiplication of proportion score (0–4) and staining intensity score (0–3). The proportion score represents the percentage of positive cells (0: no positive cells; 1: <10% of positive cells; 2: 10%–50% positive cells; 3: 51%–80% positive cells; and 4: >80% positive cells). The intensity score represents the average intensity of staining (0: no staining; 1: yellow, 2: claybank; and 3: tawny). The histologic slides were concurrently checked and scored by two blinded pathologists. The mean IRS core was considered as the final IRS of patient.

Transwell cell invasion assay

Invasion ability was evaluated by Transwell assay using 12-well Matrigel-coated Transwell chambers (BD Biosciences, San Jose, CA, USA) with a pore size of 8 μm. Briefly, upper chambers coated with Matrigel were loaded with HCCLM3 or HUH7 cells suspended in serum-free

DMEM, while lower chambers were loaded with DMEM with 10% FBS. HCCLM3 or HUH7 cells were allowed to invade through the filter for 48 hours at 37°C, and cells on the upper sides were carefully removed. Cells that invaded to the lower side were stained with 0.5% crystal violet and 4% paraformaldehyde at room temperature, and the number of penetrating cells was calculated in five random fields per membrane under an inverted microscopy at 200× magnification. Invasion assays were performed in triplicate.[32]

Wound healing cell migration analysis

HCCLM3 (5×10^5) or HUH7 (5×10^5) cells were plated into 12-well plates and grew to 60% confluence. Cells were then serum starved for 24 hours. Then, a constant wide wound was created using a 100-mL sterile pipette tip on a monolayer cultured with HCCLM3 or HUH7 cells.[33] At 48 hours after the migration of HCCLM3 or HUH7 cells, the average migrating distance to the scraped area was measured under an inverted microscope and photographed at 200× magnifications.[34] Migration analyses were performed in triplicate.

Cell counting kit-8 (CCK-8) cell proliferation assay

The proliferation ability of HCCLM3 or HUH7 cells was measured using a CCK-8 kit (Solarbio Biotechnology, Beijing, China) according to the manufacturer's instructions.[35] Briefly, HCCLM3 or HUH7 cells were seeded into 96-well plates at a density of 5×10^3 cells/well and incubated for 48 hours. Subsequently, 10 µL of CCK-8 reagent was added into the well and cultured for another 1 hour. Miniature microplate readers were used to determine the OD at 450 nm.[36] All of the experiments were performed in triplicate. The reproducibility of our study was guaranteed by repeating all experiments at least three times.

Target prediction and luciferase reporter assays

The miR-targeted proteins were predicted using the miRanda, TargetScan, and PicTar databases. A site-directed mutagenesis kit (Stratagene; Agilent Technologies, Santa Clara, CA, USA) was used to produce a mutant *UROC28* 3′-UTR luciferase reporter vector (pmirGLO-UROC28-MUT), according to the manufacturer's protocol. The luciferase reporter was composed of regions of the *UROC28* 3′-UTR with the indication of miR-431-5p target sites or mutant sites to determine whether *UROC28* was a direct target of miR-431-5p. Cells were seeded in triplicate in six-well plates and allowed to settle for 12 hours. Indicated plasmids and equal amounts of miR-431-5p or NC RNA were transfected into the cells (Thermo Fisher Scientific). At 24 hours after transfection, luciferase activity was measured using a Dual-Luciferase Reporter Assay system (Promega Corporation, Fitchburg, WI, USA).

Xenografted tumor model

The animal studies were approved by the Institutional Research Ethics Committees of The Third Affiliated Hospital of Sun Yat-Sen University. BALB/c mice (male, 6 weeks old, 20–22 g) were obtained from Vital River Laboratories (Beijing, China). All animal experiments were carried out according to the National Institutes of Health Guide for the Care and Use of Laboratory Animals. All animal study procedures in this study were also approved by the Institutional Animal Care and Use Committee (IACUC) of The Third Affiliated Hospital of Sun Yat-Sen University.[37,38] Animals were treated humanely for all experimental procedures. All animals were lawfully acquired, and their retention and use were in compliance with federal, state, and local laws and regulations and in accordance with the guidelines of the IACUC guide for care and use of laboratory animals. Immunodeficient mice were randomly divided into every group (n=6 per group). Stably transfected cells (1×10^7) were injected subcutaneously into the dorsal right flank of nude mice. The transfected cells included HCCLM3 or HUH7 HCC cells stably expressing miR-431-5p or NC miR. Tumors were examined once every week, lengths (L) and widths (W) were measured, and tumor volumes were calculated using the equation $(L \times W^2)/2$. On day 28, animals were sacrificed and tumors were harvested and weighed; tissues were used for *UROC28*, ZO-1, E-cadherin, fibronectin, N-cadherin, or GAPDH mRNA/protein quantification.

Statistical analyses

Statistical analyses were performed using SPSS 17.0 (SPSS Inc., Chicago, IL, USA). The data were presented as the mean ± SD. The two-tailed Student's t-test, Chi-squared test, Fisher's exact test, and ANOVA test were implemented to determine differences. $P<0.01$ was considered to indicate a statistically significant difference.

Results

miR-431-5p was downregulated in HCC cell lines and tissues

A real-time polymerase chain reaction (RT-PCR) assay was performed to evaluate the expression levels of miR-431-5p in

HCC cell lines HCCLM3, HUH7, Hep3B, HepG2, HLE, HLF, and SNU423, and miR-431-5p expression was found to be significantly lower in HCC cell lines, compared with the immortalized human hepatic cell line L02 ($P<0.01$, Figure 1A). Expression levels of miR-431-5p in HCC tissues and corresponding ANT were then evaluated. Results revealed that miR-431-5p expression in HCC tissues was significantly lower compared with the corresponding ANT tissues ($P<0.01$; Figure 1B). The association between miR-431-5p and the clinicopathological characteristics of several parameters of patients with HCC was analyzed preliminarily in Table S1. Then, downregulation of miR-431-5p was proved to be significantly associated with vascular invasion and tumor encapsulation deficiency by RT-PCR assay ($P<0.01$; Figure 1C and D). These findings suggest that miR-431-5p may suppress tumorigenesis and invasion in HCC.

Upregulation of miR-431-5p expression may inhibit the invasion ability of HCC cells

To further determine the role of miR-431-5p in HCC invasion, miR-431-5p was transfected into HCCLM3 or HUH7 cells to investigate the effects of miR-431-5p upregulation on the invasion of HCC cell lines. HCCLM3 cells transfected with NC miR and blank control HCCLM3 cells were used as negative and blank controls, respectively. RT-qPCR results revealed that miR-431-5p transfection significantly increased miR-431-5p expression compared with control groups at 48 hours after transfection in HCCLM3 cells ($P<0.01$; Figure 2A).

The function of miR-431-5p in HCC cells was then evaluated by measuring the cell proliferation, invasion,

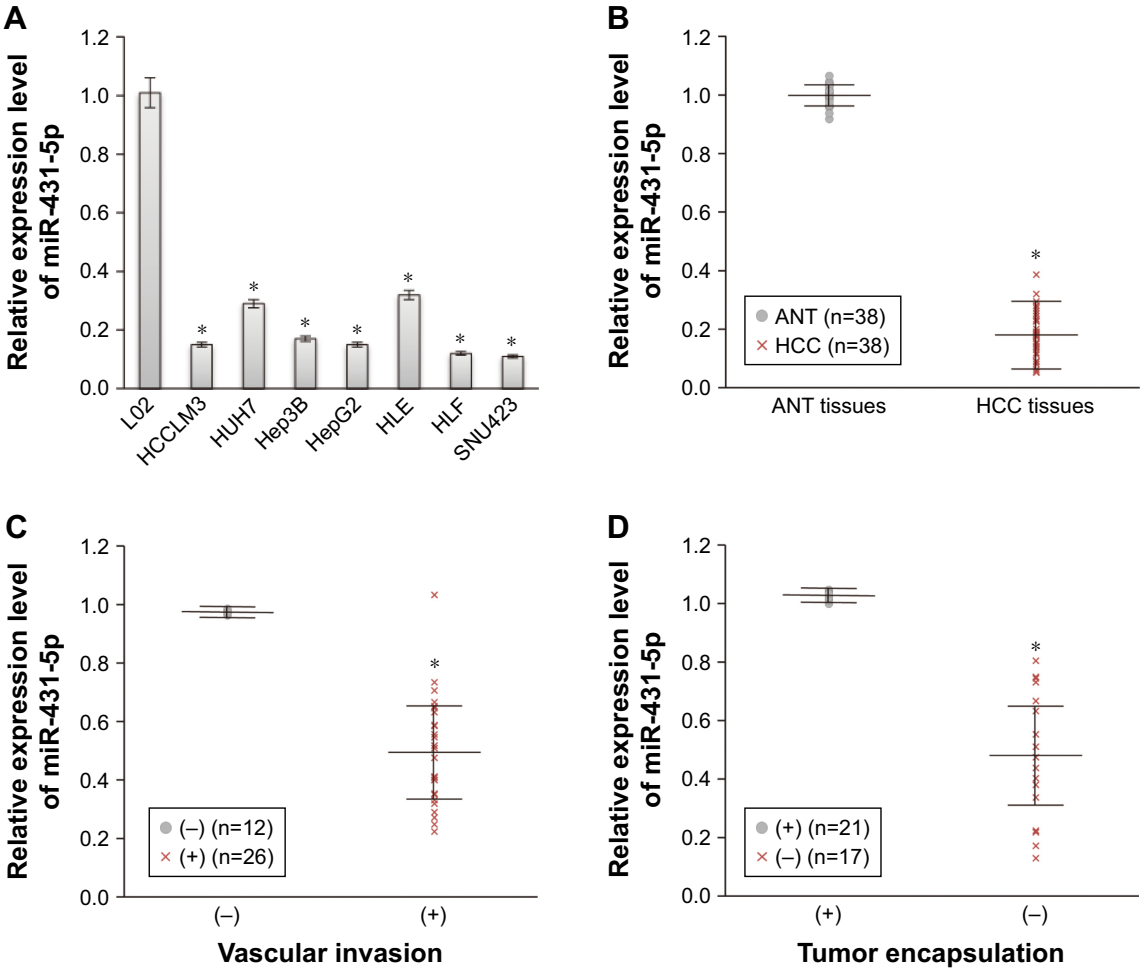

Figure 1 (**A**) Expression of miR-431-5p in the HCC cell lines HCCLM3, HUH7, Hep3B, HepG2, HLE, HLF, and SNU423 was significantly downregulated compared with the immortal liver cell line L02. (**B**) Expression levels of miR-431-5p in HCC tissues and ANT were analyzed by reverse transcription-quantitative PCR. Results revealed that miR-431-5p was significantly downregulated in HCC tissues compared with ANT. (**C**) miR-431-5p was downregulated in HCC tissues with vascular invasion compared with HCC tissues without vascular invasion. (**D**) miR-431-5p was downregulated in HCC tissues without tumor encapsulation compared with HCC tissues with tumor encapsulation. *$P<0.01$ vs HCC and miR.

Abbreviations: ANT, adjacent nontumor tissues; HCC, hepatocellular carcinoma; miR, microRNA.

and angiogenesis of HCCLM3 cells that were transfected with miR-431-5p. HCCLM3 cells transfected with NC miR or blank control HCCLM3 cells were used as negative or blank controls, respectively. First, we examined the effects of miR-431-5p on the proliferative ability of HCCLM3 cells by means of the CCK-8 assay. Results revealed that miR-431-5p upregulation significantly obstructed cell proliferation compared with control groups ($P<0.01$; Figure 2B), indicating that miR-431-5p expression could be interrelated with the proliferation potential of HCC cells. Compared with the control groups, the number of HCCLM3 cells transfected with miR-431-5p that traversed the Matrigel was significantly lower ($P<0.01$; Figure 2C). Results of a wound-healing assay further confirmed the role of miR-431-5p in the migration ability of HCCLM3 cells. The wound healing potential of HCCLM3 cells transfected with miR-431-5p was significantly inhibited compared with control groups ($P<0.01$; Figure 2D). Furthermore, tube formation assay was performed to elucidate the influence of miR-431-5p on HCC angiogenesis. Tumor cell-conditioned medium from HCCLM3 cells transfected with miR-126-3p inhibited HUVECs to form tube-like structures compared with that from control groups. Furthermore, similar results were obtained in HUH7 cells (Figure 2B and E). Thus, we can conclude that miR-431-5p is an important factor in the proliferation, invasion, and angiogenesis of HCC cells.

Upregulation of miR-431-5p expression may alter the EMT markers in HCC cells

Previous studies have reported that some miRs can promote invasion by mediating the EMT. In order to evaluate the role of miR-431-5p in inducing the EMT in HCC, mRNA and protein expression levels of the epithelial markers ZO-1 and E-cadherin[39,40] and the mesenchymal markers fibronectin and N-cadherin[41] in HCCLM3 cells were measured by RT-PCR or Western blotting. As presented in Figure 3A and B, upregulation of miR-431-5p in HCCLM3 cells resulted in significant upregulation of the mRNA and protein expression of ZO-1 and E-cadherin compared with control groups ($P<0.01$), while the expression levels of

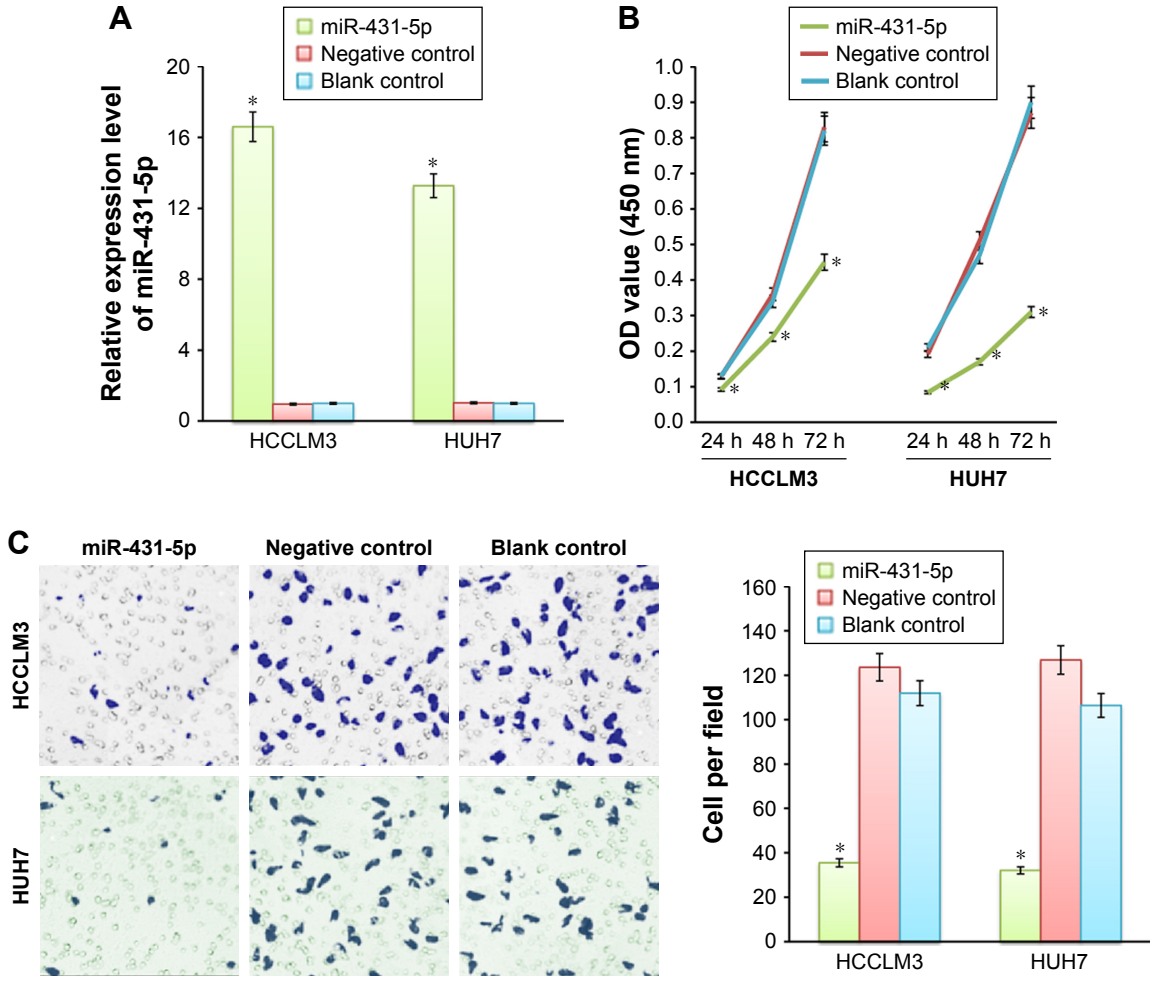

Figure 2 (*Continued*)

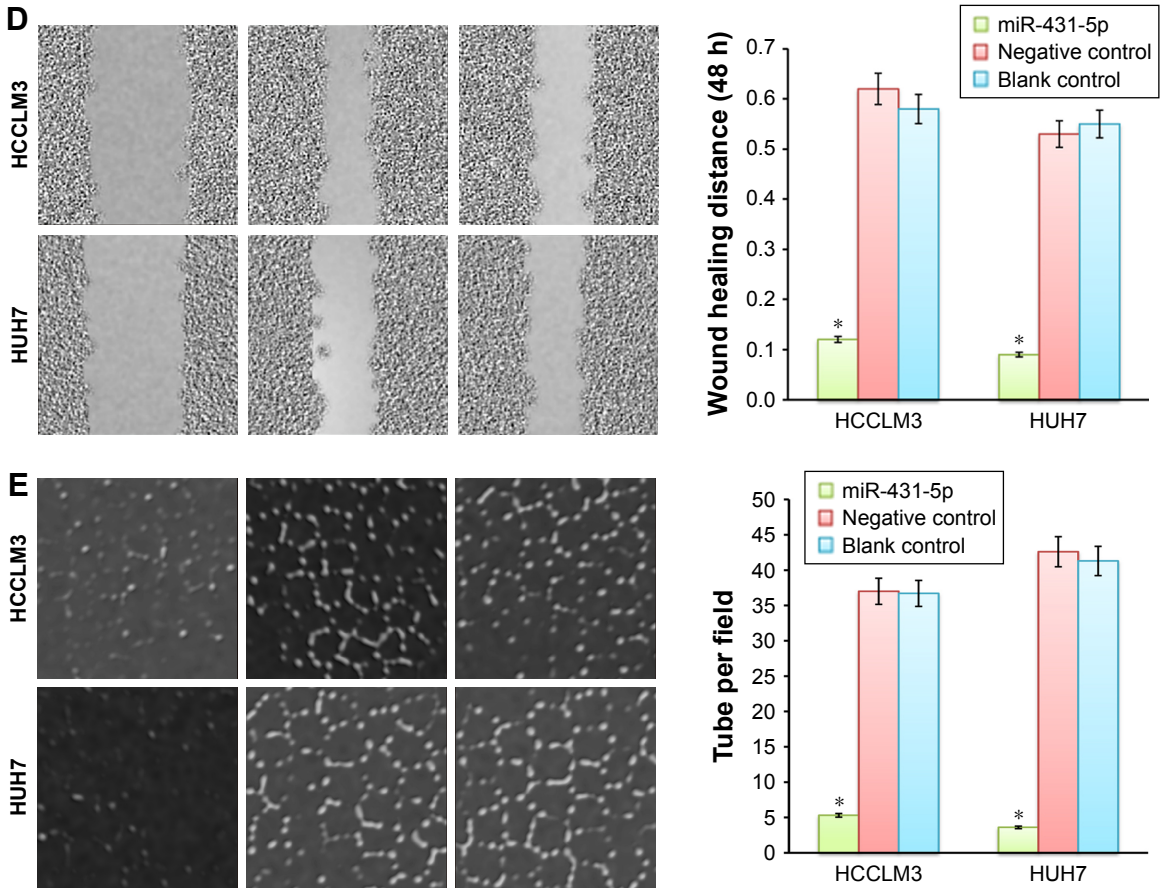

Figure 2 Upregulation of miR-431-5p inhibited the proliferation, invasion, migration, and angiogenesis of hepatocellular carcinoma cells.
Notes: Transfection with miR-431-5p significantly increased the expression of miR-431-5p in (**A**) HCCLM3 and HUH7 cells compared with cells transfected with NC miR or blank control cells. (**B**) A cell counting kit-8 assay was used to examine the proliferative ability of HCCLM3 and HUH7 cells at 24, 48 and 72 hours after transfection with miR-431-5p. (**C**) Results of a Transwell assay revealed that upregulation of miR-431-5p significantly downregulated the number of HCCLM3 and HUH7 cells that invaded through the membrane compared with blank control cells (200× magnification). (**D**) Upregulation of miR-431-5p also significantly decreased the wound healing migration distance of HCCLM3 and HUH7 cells compared with blank control cells (200× magnification). (**E**) Upregulation of miR-431-5p significantly decreased the vascular tube forming ability of HUVECs cultured on Matrigel-coated plates with conditioned media from the indicated groups of HCCLM3 and HUH7 cells compared with blank control cells (100× magnification). HCCLM3 or HUH7 transfected with NC miR or blank control cells were used as negative or blank controls, respectively (n=3, *$P<0.01$ vs blank control cells).
Abbreviations: HUVECs, human umbilical vein endothelial cells; NC, negative control.

fibronectin and N-cadherin were significantly decreased compared with the control groups ($P<0.01$). In addition, similar results were revealed in HUH7 cells (Figure 3A and B). Thus, miR-431-5p was concluded to be capable of promoting invasion by adjusting the EMT markers in HCC cells. As a result, miR-431-5p could be targeted in order to regulate EMT-associated invasion.

UROC28 was directly targeted by miR-431-5p via the 3′-UTR

Although the major function of miR-431-5p in the development of diffuse large B-cell lymphoma, hepatocellular cancer, and bladder cancers, as well as many other cancers, has been previously demonstrated,[10] the mechanism by which miR-431-5p is able to promote invasion has not been examined explicitly in HCC. *UROC28*, a tumor promoter, is known to regulate the promotion of cell proliferation, colony formation, and metastasis elevation.[20] Upregulation of *UROC28* has been identified in numerous different cancer types, including breast, prostate, and bladder cancers, with the tendency to promote the development of cancer cells.[23] By using PicTar and TargetScan software, miR-431-5p was revealed to have an assumed binding site in the 3′-UTR of *UROC28*. In order to confirm whether *UROC28* was a functional target of miR-431-5p, NC miR or miR-431-5p was cotransfected with pmirGLO-UROC28-WT or pmirGLO-UROC28-MUT in HCC cells. As shown in Figure 4A, HCC cells co-transfected with miR-431-5p and pmirGLO-UROC28-WT presented a statistically significant decrease in reporter activity compared with HCC cells cotransfected with NC miR and pmirGLO-UROC28-WT ($P<0.01$). Furthermore, HCC cells cotransfected with

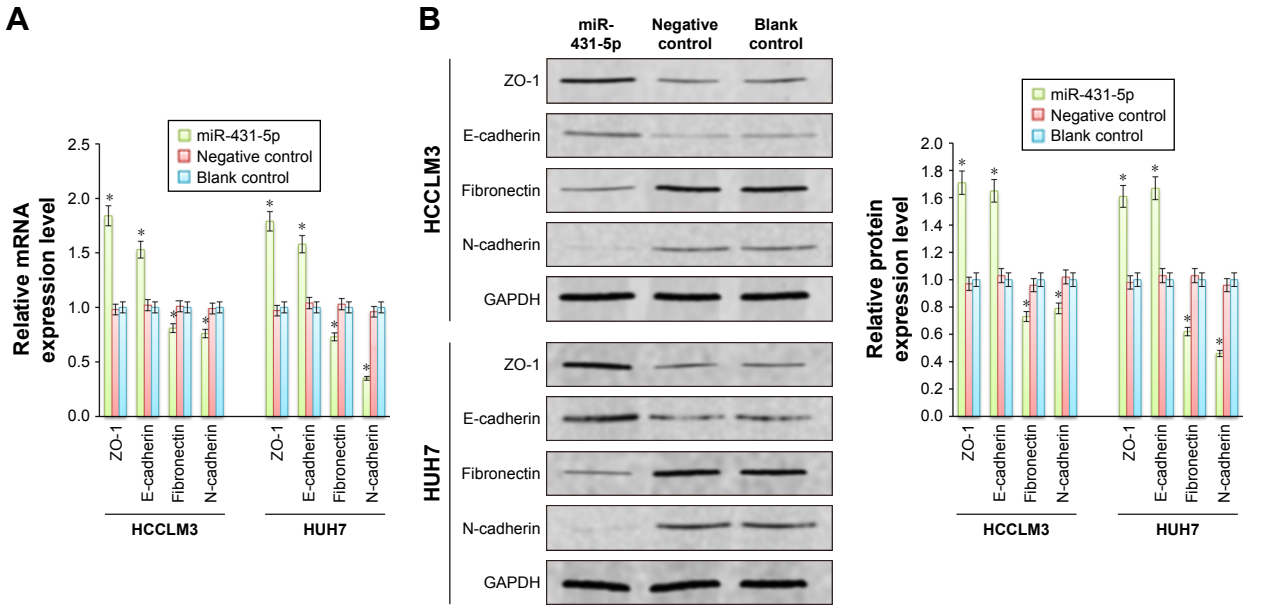

Figure 3 Upregulation of miR-431-5p altered the expression level of the EMT markers in hepatocellular carcinoma cells.
Notes: RT-PCR and Western blot assay were used to detect the (**A**) mRNA and (**B**) protein expression levels of the epithelial markers ZO-1 and E-cadherin and the mesenchymal markers fibronectin and N-cadherin in HCCLM3 or HUH7 cells. Results revealed that mRNA and protein expression levels of ZO-1 and E-cadherin were upregulated in the miR-431-5p group compared with control groups, while the mRNA and protein expression levels of fibronectin and N-cadherin were downregulated in HCCLM3 or HUH7 cells treated with miR-431-5p compared with control groups (n=3, *$P<0.01$ vs blank control cells).
Abbreviation: EMT, epithelial-to-mesenchymal transition.

miR-431-5p and pmirGLO-UROC28-MUT or NC miR with pmirGLO-UROC28-MUT demonstrated no significant change in reporter activity ($P>0.01$). Thus, the luciferase activity of the wild-type UROC28-3′-UTR but not the mutated UROC28-3′-UTR reporter was reduced by miR-431-5p in HCC cells. In order to further confirm the regulatory effects of miR-431-5p on *UROC28*, RT-qPCR and Western blot analysis were used to check expression levels of *UROC28* in different groups of cells. Results revealed that upregulation of miR-431-5p in HCCLM3 or HUH7 cells resulted in significant downregulation of mRNA and protein expression of *UROC28* ($P<0.01$; Figure 4B and C). However, the mRNA and protein expression of *UROC28* in HCCLM3 or HUH7 cells transfected with NC miR demonstrated no significant difference compared with blank control HCCLM3 or HUH7 cells (Figure 4B and C). To further determine the expression level of *UROC28* protein in HCC, Western blotting assay was conducted in pairs of clinical specimens. Upregulation of *UROC28* protein levels was detected in the tissue sections of HCC tissues in all specimens. Typically, the *UROC28* expression level in the HCC tissue samples was significantly increased compared with that in the ANT from the same patient (Figure 4D). At the same time, inverse correlation between expression levels of miR-431-5p and *UROC28* protein was also demonstrated by retrospective analysis on clinical-pathology data ($P<0.01$, Table S1). These results indicate that miR-431-5p may directly regulate *UROC28* expression by binding to the 3′-UTR of *UROC28* in HCCLM3 or HUH7 HCC cells.

Upregulation of *UROC28* partially increased the invasion ability of HCC cells

UROC28 has been reported to participate in proliferation and invasion in cancer cells.[21,22] In order to evaluate whether miR-431-5p participates in the invasion of HCC by regulating the expression of *UROC28*, the pCMV-UROC28 eukaryotic expression vector was synthesized and cotransfected into HCCLM3 or HUH7 cells together with miR-431-5p. The three control groups were as follows: the *UROC28* expression vector cotransfected with NC miR; the *UROC28* expression vector transfected into HCCLM3 or HUH7 cells alone; or blank control HCCLM3 or HUH7 cells. In HCCLM3 cells, expression levels of *UROC28* were significantly upregulated in the *UROC28* expression vector-transfected group compared with the untransfected group ($P<0.01$; Figure 5A and B). In addition, expression levels of *UROC28* were significantly upregulated in the pCMV-UROC28 vector and miR-431-5p cotransfected group compared with the miR-431-5p alone transfected group ($P<0.01$; Figure 5A and B). A Boyden chamber invasion assay and a wound healing assay were used again to evaluate the invasive ability of HCCLM3 cells between different groups. A significant increase in invasion was identified in

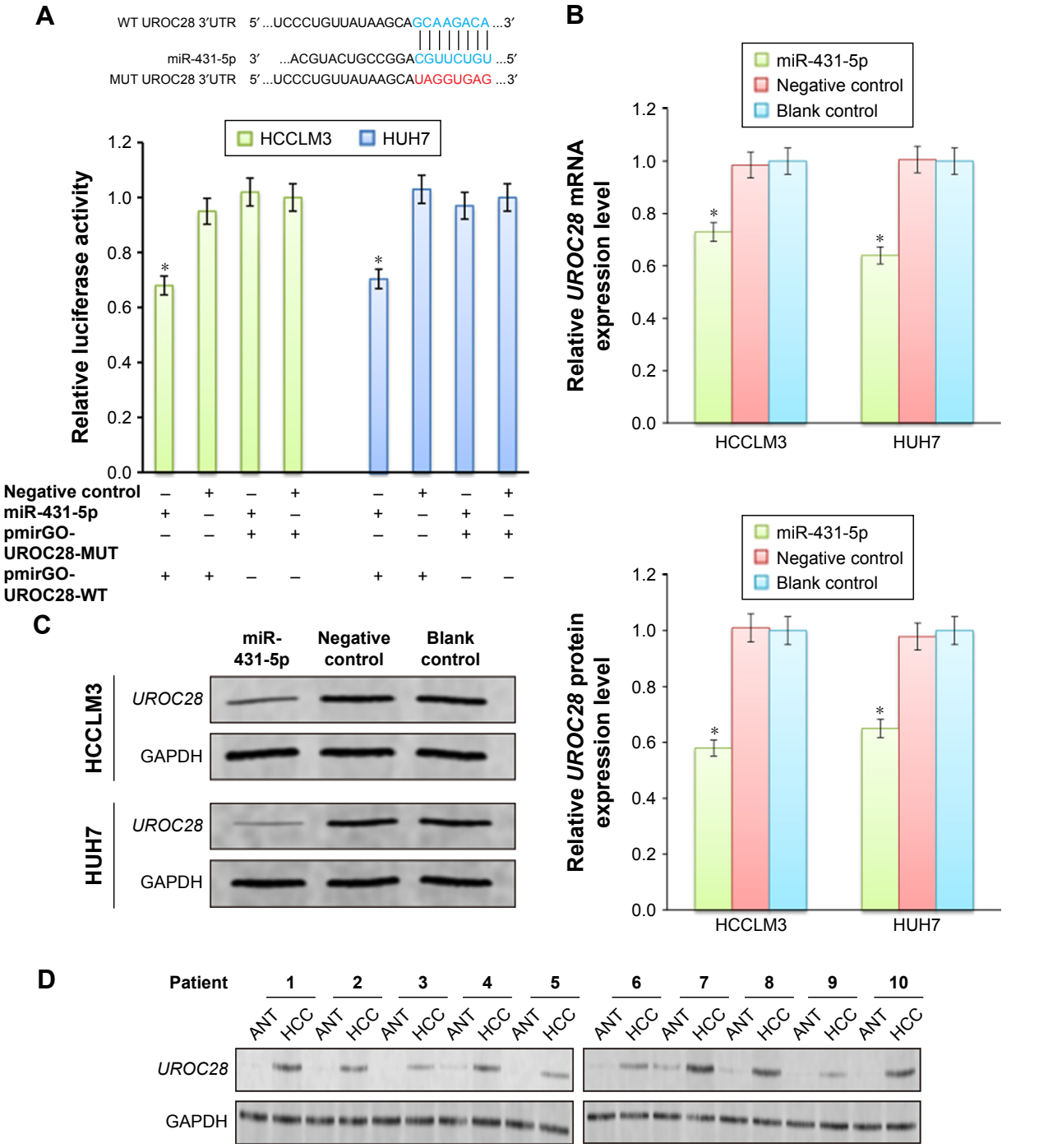

Figure 4 *UROC28* was directly targeted by miR-431-5p via the 3′-UTR.

Notes: (**A**) A luciferase activity assay was used to determine the reporter activity in HCCLM3 or HUH7 cells cotransfected with either miR-431-5p mimics or negative control miR and either pmirGLO-UROC28-WT or pmirGLO-UROC28-MUT. The mutant miR-431-5p-binding site was generated in the complementary site for the seed region of miR-431-5p (n=3, *$P<0.01$ vs the negative control miR and pmirGLO-UROC28-MUT cotransfected cells). Subsequently, the relative (**B**) mRNA and (**C**) protein expression levels of *UROC28* in HCCLM3 or HUH7 cells with or without miR-431-5p were determined (n=3, *$P<0.01$ vs blank control cells). (**D**) Protein expression levels of *UROC28* in HCC tissues and paired adjacent nontumor liver tissues from the same patient were analyzed by Western blotting assay. GAPDH was used as an internal control.

Abbreviation: HCC, hepatocellular carcinoma.

the pCMV-UROC28 vector and miR-431-5p-transfected group in HCCLM3 or HUH7 cells, compared with the miR-431-5p alone transfected group ($P<0.01$; Figure 5C and D). In addition, upregulation of *UROC28* may partially rescue the invasive ability of HCCLM3 cells (evaluated by using the Transwell assay and wound healing assay), as significant differences were identified in the *UROC28* eukaryotic expression vector-transfected groups ($P<0.01$) and the *UROC28* eukaryotic expression vector- and miR-431-5p-transfected groups ($P<0.01$) in HCCLM3 cells

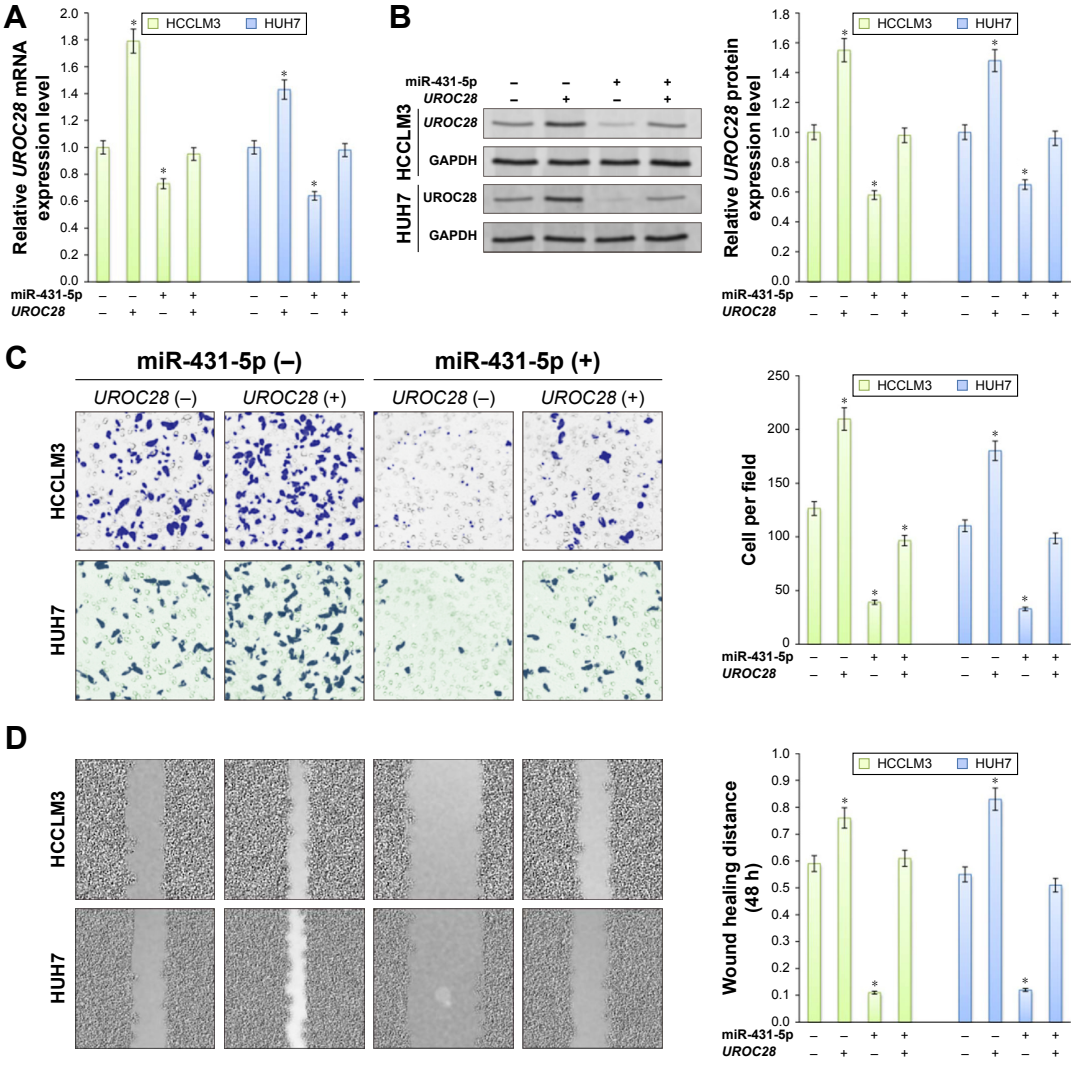

Figure 5 Upregulation of *UROC28* partially increased the invasion of hepatocellular carcinoma cells.
Notes: Transfection of pCMV-UROC28 can rescue the miR-431-5p-induced reduction in (**A**) mRNA and (**B**) protein expression levels of *UROC28* in HCCLM3 or HUH7 cells. The invasion (**C**) and the migration ability (**D**) of HCCLM3 or HUH7 cells were examined by a Transwell assay and a wound healing assay, respectively. Transfection of pCMV-UROC28 also rescued the miR-431-5p-induced reduction in invasion (n=3, *$P<0.01$ vs untransfected cells).

(Figure 5C and D). In HUH7 cells, upregulation of *UROC28* also rescued the invasive and metastatic properties of HUH7 cells that were inhibited by miR-431-5p (Figure 5C and D). Taken together, miR-431-5p is possibly a crucial regulator in the invasion of HCC, which may occur via the regulation of *UROC28* expression.

Upregulation of *UROC28* partially rescued expression of the EMT markers in HCC cells. miRs affect the EMT markers by influencing the expression of target proteins and signaling pathways. *UROC28* has a notable function in tumor invasion and migration; *UROC28* is often overexpressed in many kinds of cancer types and is associated with the cancer EMT process.[18] As previously suggested, miR-431-5p regulates the expression of *UROC28* by binding to its promoter. However, whether *UROC28* contributes to the miR-431-5p-induced EMT marker regulation in HCC remains to be clarified. In the current study, it was discovered that upregulation of *UROC28* in HCCLM3 or HUH7 cells partially rescued the influence of the EMT markers by upregulated expression of miR-431-5p. The mRNA and protein expression levels of ZO-1 and E-cadherin in HCCLM3 cells were significantly upregulated, and fibronectin and N-cadherin levels were significantly downregulated in cells transfected with *UROC28* eukaryotic expression vector alone compared with untransfected cells ($P<0.01$) and in cells transfected with *UROC28* eukaryotic expression vector and miR-431-5p compared with cells transfected with miR-431-5p alone ($P<0.01$; Figure 6A and B). Similar results were demonstrated in HUH7 cells (Figure 6A and B). In conclusion, the results of the current study reveal that miR-431-5p influenced the EMT markers by inhibiting *UROC28* expression.

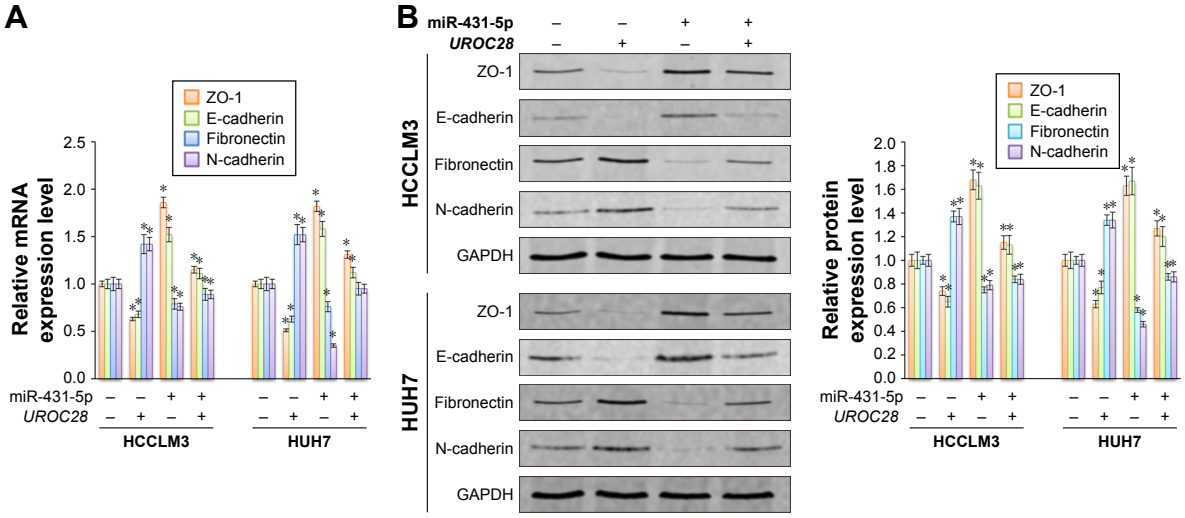

Figure 6 Upregulation of *UROC28* partially rescued the EMT markers influenced by the upregulation of miR-431-5p.
Notes: Results of the RT-PCR assay and Western blot assay were used to determine the (**A**) mRNA and (**B**) protein expression levels of Zonula Occludens protein-1 (ZO-1) and E-cadherin and fibronectin and N-cadherin in HCCLM3 or HUH7 cells that were untransfected, transfected with either *UROC28* eukaryotic expression vector or miR-431-5p alone, or cotransfected (n=3, *$P<0.01$ vs untransfected cells).
Abbreviations: EMT, epithelial-to-mesenchymal transition; ZO-1, Zonula Occludens protein-1.

miR-431-5p suppresses hepatocellular cancer xenograft growth in vivo

In order to further confirm the tumor-suppressing activity of miR-431-5p in hepatic cancers, we formed a xenograft model to explore the effects of miR-431-5p on tumor growth (Figure 7). HCCLM3 or HUH7 cells with the upregulated expression of miR-431-5p or NC were implanted into nude mice (4 weeks). Mice were sacrificed at 28 days after the injection of tumor cells. The growth rates of the HCCLM3 or HUH7 tumors were measured by tumor volume. Tumor growth was significantly suppressed by the upregulation of miR-431-5p (Figure 7A and B). Thus, these results indicated that miR-431-5p has a function of growth suppression in hepatic cancer in vivo. To further determine whether this suppressive effect in HCC is accompanied by a reduction of *UROC28* protein expression and a regulation of EMT markers in vivo, we used Western blotting experiments and IHC assay to detect the expression of *UROC28*, ZO-1, E-cadherin, fibronectin, and N-cadherin proteins in HCCLM3 and HUH7 tumor tissues. We found that *UROC28* and the mesenchymal markers fibronectin and N-cadherin were significantly decreased and the epithelial markers ZO-1 and E-cadherin were increased in miR-431-5p-upregulated HCCLM3 or HUH7 tumors by Western blotting assay ($P>0.01$, Figure 7C).

In addition, the IHC assay of HCCLM3 tumor tissue was carried out. The protein expression levels of *UROC28* and EMT markers showed the same change trend as the Western blot results by IHC assay (Figure 7D). In summary, the results of the in vivo experiments supported the in vitro experimental results and showed that miR-431-5p plays a significant role in suppressing the invasive ability via regulating the EMT markers of HCC cells in vitro and in vivo.

Discussion

microRNAs (miRs), small non-coding RNAs of ~22 nucleotides in length, are small RNAs that are involved in the posttranscriptional regulation of gene expression.[42,43] miRs have been demonstrated to be associated with the occurrence and development of human cancer, by behaving as tumor suppressors or oncogenes.[44] The association between miR deregulation and cancer has led many scientists to do a lot of research to clarify the role of miRs in various cancers. More and more research results support the idea that aberrant of miR expression level is the rule rather than the exception in cancer development. miRs are participated in the regulation of virtually all cancer-relevant processes, such as proliferation, apoptosis, and migration and invasion.[45] Apart from cancer, miRs are found to be associated with an increasing number of other diseases, such as metabolic disorders and infectious diseases.[46] Previous studies have demonstrated the abnormal expression levels of numerous miRs in HCC including miR-431. miR-431-5p is a member of the miR-431 cluster, and it has been demonstrated to be downregulated in a number of different types of cancer, including hepatocellular cancer, bladder cancer, diffuse large B-cell lymphoma, and lung cancer.[10,12,14,16,47] However, the function and mechanism of miR-431-5p in HCC have not been elucidated. Pan et al[10] revealed that the downregulation of miR-431 was partially responsible for a series

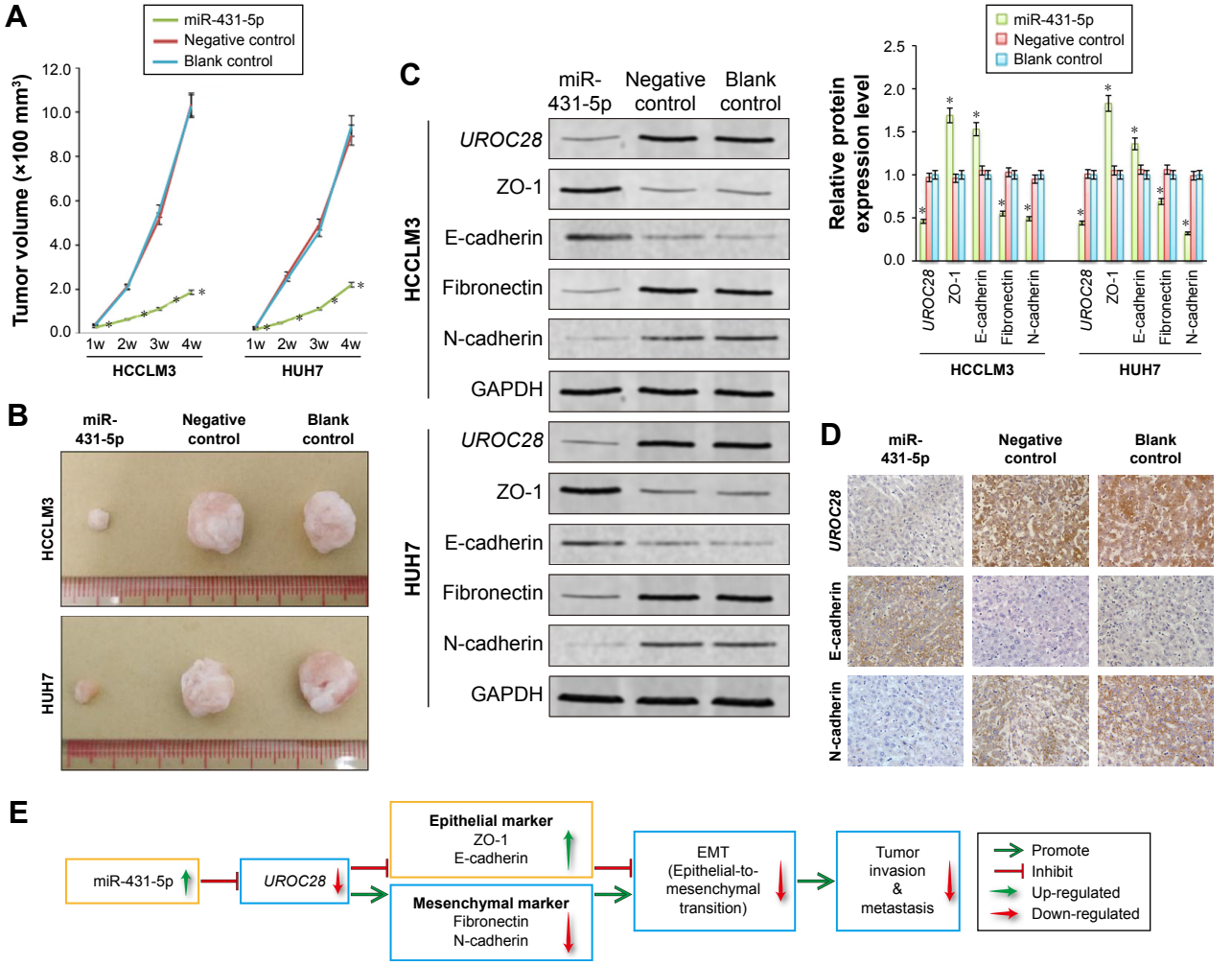

Figure 7 The therapeutic effect of upregulation of miR-431-5p on HCC cells in vivo.

Notes: (**A**) Upregulation of miR-431-5p inhibited the growth of HCCLM3 and HUH7 HCC cell xenograft models. (**B**) Tumor volume was measured on day 28 of the experiment. (**C**) Protein expressions of *UROC28*, ZO-1, E-cadherin, fibronectin, or N-cadherin in xenograft tumors of nude mice detected by Western blotting (n=6, *$P<0.01$ vs blank control groups). (**D**) Protein expression levels of *UROC28*, E-cadherin, or N-cadherin in xenograft tumors detected by IHC staining. (**E**) Schematic diagram of possible therapeutic mechanism of miR-431-5p in HCC.

Abbreviations: HCC, hepatocellular carcinoma; IHC, immunohistochemistry.

of clinicopathological features and could be tightly correlated with the progression of HCC patients. Furthermore, Sun et al[16] reported that downregulation of miR-431 was prominently associated with poor prognostic features of HCC patients and suggested that miR-431 may inhibit the migration and invasion of HCC cells in vitro. However, the above findings have not been confirmed by persuasive data generated from luciferase reporter assays and in vivo studies.

In the present study, expression levels of miR-431-5p in HCC tissues were shown to be significantly lower compared with corresponding ANT. Moreover, a significant association was also demonstrated between the expression levels of miR-431-5p and vascular invasion and deficiency tumor encapsulation, indicating that the expression of miR-431-5p also had a notable function in HCC invasion. Consistent with the data that were investigated in HCC tissues, it was further verified that expression levels of miR-431-5p in the HCC cell lines HCCLM3, HUH7, Hep3B, HepG2, HLE, HLF, and SNU423 were also significantly lower compared with the immortalized liver cell line L02, suggesting that the downregulation of miR-431-5p may promote the initiation and development of HCC.

To further illuminate the role of miR-431-5p in the initiation and development of HCC, miR-431-5p and NC miR were individually transfected into HCCLM3 or HUH7 cells using a lentiviral transfection system and blank control HCCLM3 or HUH7 cells were used as the blank control groups. Expression levels of miR-431-5p increased significantly in HCCLM3 or HUH7 cells transfected with miR-431-5p compared with

those transfected with NC miR or blank control HCCLM3 or HUH7 cells. Increasing the expression of miR-431-5p significantly reduced the proliferation and invasion of HCCLM3 or HUH7 cells compared with those transfected with NC miR or blank control HCCLM3 or HUH7 cells. These results further validate the clinicopathological data that miR-431-5p may play a role in inhibiting proliferation and invasion in HCC cells. The EMT process serves a fundamental function in HCC invasion. Developing evidence has disclosed that miRs are involved in regulating the EMT in numerous types of cancer cells. Moreover, Fang et al[6] indicated that miR-431 may interact with the mesenchymal marker fibronectin and N-cadherin in HepG2 cells. In the present study, it was demonstrated that by upregulating miR-431-5p, the mRNA and protein expression levels of the epithelial markers ZO-1 and E-cadherin[48] significantly increased, while the expression of the mesenchymal markers fibronectin and N-cadherin[49] significantly decreased. Therefore, it was concluded that miR-431-5p potentially contributes to the invasion process of HCC cells by regulating the EMT markers.

In previous years, *UROC28* has been widely viewed as an oncogene, which regulates initiation and development in various cancer types. *UROC28* may activate tumors by regulating cell cycle inhibitors and the Hedgehog signaling pathway.[22] miRs always function through binding to the 3′UTRs of their target genes,[8] and numerous previous reports have confirmed that miR-431-5p plays an important role in various cancer types including HCC cells.[6] In the present study, it was demonstrated that miR-431-5p upregulation may result in the decreased expression level of *UROC28* in HCC cells compared with control cells. Using cell transfection and luciferase reporter assays, it was also revealed that *UROC28* was a direct target gene of miR-431-5p. It was shown that the rescue expression of *UROC28* by the eukaryotic expression vector in HCCLM3 or HUH7 cells transfected with miR-431-5p may partially reverse the effects on invasion caused by miR-431-5p upregulation. Furthermore, upregulation of *UROC28* partially rescued the miR-431-5p-induced changes in the EMT markers. These results also demonstrated that miR-431-5p inhibited the invasion of HCC cells via altering of the UROC28-mediated EMT markers. To further clarify the role of miR-431-5p in HCC, in vivo studies were conducted. In vivo experiments demonstrated that the growth rates of subcutaneous tumors were inhibited by the upregulation of miR-431-5p. Moreover, expression levels of the miR-431-5p-targeted protein *UROC28* and EMT markers were confirmed to have a similar tendency as the in vitro studies. Therefore, our study has provided strong evidence highlighting the novel regulatory axis of miR-431-5p/*UROC28* in the development of HCC (Figure 7E).

Conclusion

The results of the present study showed that miR-431-5p was downregulated in HCC cell lines and tissues, particularly in HCC tissues with vascular invasion and deficiency tumor encapsulation. Furthermore, it was demonstrated that the function of miR-431-5p in HCC was dependent on regulating the UROC28-mediated EMT markers. Therefore, the miR-431-5p/*UROC28* axis may be a potential molecular target for treating HCC. Increasing levels of miR-431-5p could be a candidate therapeutic technique for HCC patients.

Acknowledgments

This study was supported by the Science and Technology Project of Guangdong Province (No 2014A020212533) and the Special Project of Collaboration and Innovation of Guangzhou City (201704020049). The funders had no role in study design, data collection and analysis, decision to publish, or preparation of the manuscript.

Disclosure

The authors report no conflicts of interest in this work.

References

1. Zheng C, Zeng H, Lin H, et al. Serum microcystin levels positively linked with risk of hepatocellular carcinoma: A case-control study in southwest China. *Hepatology*. 2017;66(5):1519–1528.
2. Ye X, Guo Y, Zhang Q, et al. βKlotho suppresses tumor growth in hepatocellular carcinoma by regulating Akt/GSK-3β/cyclin D1 signaling pathway. *PLoS One*. 2013;8(1):e55615.
3. Toy M, Salomon JA, Jiang H, et al. Population health impact and cost-effectiveness of monitoring inactive chronic hepatitis B and treating eligible patients in Shanghai, China. *Hepatology*. 2014;60(1):46–55.
4. Zhang T, Liu W, Zeng XC, et al. Down-regulation of microRNA-338-3p promoted angiogenesis in hepatocellular carcinoma. *Biomed Pharmacother*. 2016;84:583–591.
5. Che X, Huang C. microRNA, Cancer and Cancer Chemoprevention. *Curr Mol Pharmacol*. 2012;5(2):402–418.
6. Fang L, Du WW, Yang X, et al. Versican 3′-untranslated region (3′-UTR) functions as a ceRNA in inducing the development of hepatocellular carcinoma by regulating miRNA activity. *FASEB J*. 2013;27(3):907–919.
7. Cai S, Chen R, Li X, et al. Downregulation of microRNA-23a suppresses prostate cancer metastasis by targeting the PAK6-LIMK1 signaling pathway. *Oncotarget*. 2015;6(6):3904–3917.
8. Ye Z, Shen N, Weng Y, et al. Low miR-145 silenced by DNA methylation promotes NSCLC cell proliferation, migration and invasion by targeting mucin 1. *Cancer Biol Ther*. 2015;16(7):1071–1079.
9. Torres-Martin M, Lassaletta L, de Campos JM, et al. Global profiling in vestibular schwannomas shows critical deregulation of microRNAs and upregulation in those included in chromosomal region 14q32. *PLoS One*. 2013;8(6):e65868.

10. Pan L, Ren F, Rong M, et al. Correlation between down-expression of miR-431 and clinicopathological significance in HCC tissues. *Clin Transl Oncol*. 2015;17(7):557–563.
11. Rapa I, Votta A, Felice B, et al. Identification of MicroRNAs Differentially Expressed in Lung Carcinoid Subtypes and Progression. *Neuroendocrinology*. 2015;101(3):246–255.
12. Tanaka T, Arai M, Jiang X, et al. Downregulation of microRNA-431 by human interferon-β inhibits viability of medulloblastoma and glioblastoma cells via upregulation of SOCS6. *Int J Oncol*. 2014;44(5):1685–1690.
13. Yamaguchi N, Osaki M, Onuma K, et al. Identification of MicroRNAs Involved in Resistance to Sunitinib in Renal Cell Carcinoma Cells. *Anticancer Res*. 2017;37(6):2985–2992.
14. Meng Y, Quan L, Liu A. Identification of key microRNAs associated with diffuse large B-cell lymphoma by analyzing serum microRNA expressions. *Gene*. 2018;642:205–211.
15. Trehanpati N, Sehgal R, Patra S, et al. miRNA signatures can predict acute liver failure in hepatitis E infected pregnant females. *Heliyon*. 2017;3(4):e287.
16. Sun K, Zeng T, Huang D, et al. MicroRNA-431 inhibits migration and invasion of hepatocellular carcinoma cells by targeting the ZEB1-mediated epithelial-mesenchymal transition. *FEBS Open Bio*. 2015;5:900–907.
17. Kamagata C, Tsuji N, Kondoh K, et al. Enhanced expression of the UROC28 gene in human breast cancer: relationship to ERBB2 gene expression. *Anticancer Res*. 2002;22(6C):4087–4091.
18. Guo Y, Wu Z, Shen S, et al. Nanomedicines reveal how PBOV1 promotes hepatocellular carcinoma for effective gene therapy. *Nat Commun*. 2018;9(1):3430.
19. Wong N, Wang X. miRDB: an online resource for microRNA target prediction and functional annotations. *Nucleic Acids Res*. 2015;43(Database issue):D146–D152.
20. Wang L, Niu CH, Wu S, et al. PBOV1 correlates with progression of ovarian cancer and inhibits proliferation of ovarian cancer cells. *Oncol Rep*. 2016;35(1):488–496.
21. Pan T, Wu R, Liu B, et al. PBOV1 promotes prostate cancer proliferation by promoting G1/S transition. *Onco Targets Ther*. 2016;9:787–795.
22. Samusik N, Krukovskaya L, Meln I, Shilov E, Kozlov AP. PBOV1 is a human de novo gene with tumor-specific expression that is associated with a positive clinical outcome of cancer. *PLoS One*. 2013;8(2):e56162.
23. Carleton NM, Zhu G, Gorbounov M, et al. PBOV1 as a potential biomarker for more advanced prostate cancer based on protein and digital histomorphometric analysis. *Prostate*. 2018;78(7):547–559.
24. Jiang WY, Zhou BY, Yu GL, et al. G6PD genotype and its associated enzymatic activity in a Chinese population. *Biochem Genet*. 2012;50(1–2):34–44.
25. Li J, Ou Z, Wang F, et al. Distinctiveness of the cagA genotype in children and adults with peptic symptoms in South China. *Helicobacter*. 2009;14(4):248–255.
26. Wu Z, Zhao J, Qiu M, et al. CRISPR/Cas9 mediated GFP knock-in at the MAP1LC3B locus in 293FT cells is better for bona fide monitoring cellular autophagye1700674. *Biotechnol J*. Epub 2018 Apr 19.
27. Lin S, Feng S, Mo Y, et al. Dual-responsive crosslinked micelles of a multifunctional graft copolymer for drug delivery applications. *J Polym Sci A Polym Chem*. 2017;55(9):1536–1546.
28. Guo Y, Chen W, Wang W, et al. Simultaneous diagnosis and gene therapy of immuno-rejection in rat allogeneic heart transplantation model using a T-cell-targeted theranostic nanosystem. *ACS Nano*. 2012;6(12):10646–10657.
29. Guo Y, Liang X, Lu M, Weng T, Liu Y, Ye X. Mammalian target of rapamycin as a novel target in the treatment of hepatocellular carcinoma. *Hepatogastroenterology*. 2010;57(101):913–918.
30. Guo Y, Wang J, Zhang L, et al. Theranostical nanosystem-mediated identification of an oncogene and highly effective therapy in hepatocellular carcinoma. *Hepatology*. 2016;63(4):1240–1255.
31. Guo Y, Wang J, Li H, et al. Mediator subunit 23 overexpression as a novel target for suppressing proliferation and tumorigenesis in hepatocellular carcinoma. *J Gastroenterol Hepatol*. 2015;30(6):1094–1103.
32. Wang C, Guo Y, Wang J, Min Z. Annexin A2 knockdown inhibits hepatoma cell growth and sensitizes hepatoma cells to 5-fluorouracil by regulating β-catenin and cyclin D1 expression. *Mol Med Rep*. 2015;11(3):2147–2152.
33. Wang C, Guo Y, Wang J, Min Z. The suppressive role of SOX7 in hepatocarcinogenesis. *PLoS One*. 2014;9(5):e97433.
34. Wang J, Ou J, Guo Y, et al. TBLR1 is a novel prognostic marker and promotes epithelial-mesenchymal transition in cervical cancer. *Br J Cancer*. 2014;111(1):112–124.
35. Chen Z, Xu L, Su T, et al. Autocrine STIP1 signaling promotes tumor growth and is associated with disease outcome in hepatocellular carcinoma. *Biochem Biophys Res Commun*. 2017;493(1):365–372.
36. Wu YF, Liang XJ, Liu YY, et al. +Antisense oligonucleotide targeting survivin inhibits growth by inducing apoptosis in human osteosarcoma cells MG-63. *Neoplasma*. 2010;57(6):501–506.
37. Guo RM, Li QL, Zhong LR, et al. Brain MRI findings in acute hepatic encephalopathy in liver transplant recipients. *Acta Neurol Belg*. 2018;118(2):251–258.
38. Guo R, Li Q, Yang F, et al. In Vivo MR Imaging of Dual MRI Reporter Genes and Deltex-1 Gene-modified Human Mesenchymal Stem Cells in the Treatment of Closed Penile Fracture. *Mol Imaging Biol*. 2017;20(3):417–427.
39. Vandewalle C, Comijn J, De Craene B, et al. SIP1/ZEB2 induces EMT by repressing genes of different epithelial cell-cell junctions. *Nucleic Acids Res*. 2005;33(20):6566–6578.
40. Xiao X, Tang W, Yuan Q, Peng L, Yu P. Epigenetic repression of Krüppel-like factor 4 through Dnmt1 contributes to EMT in renal fibrosis. *Int J Mol Med*. 2015;35(6):1596–1602.
41. Chen H, Pan J, Zhang L, et al. Downregulation of estrogen-related receptor alpha inhibits human cutaneous squamous cell carcinoma cell proliferation and migration by regulating EMT via fibronectin and STAT3 signaling pathways. *Eur J Pharmacol*. 2018;825:133–142.
42. Ye Z, Hao R, Cai Y, Wang X, Huang G. Knockdown of miR-221 promotes the cisplatin-inducing apoptosis by targeting the BIM-Bax/Bak axis in breast cancer. *Tumour Biol*. 2016;37(4):4509–4515.
43. Ye Z, Yin S, Su Z, et al. Downregulation of miR-101 contributes to epithelial-mesenchymal transition in cisplatin resistance of NSCLC cells by targeting ROCK2. *Oncotarget*. 2016;7(25):37524–37535.
44. Wei Y, Zhou W, Li X, Chai Y, Yuan R, Xiang Y. Coupling hybridization chain reaction with catalytic hairpin assembly enables non-enzymatic and sensitive fluorescent detection of microRNA cancer biomarkers. *Biosens Bioelectron*. 2016;77:416–420.
45. Yuan H-L, Wang T, Zhang K-H. MicroRNAs as potential biomarkers for diagnosis, therapy and prognosis of gastric cancer. *Onco Targets Ther*. 2018;11:3891–3900.
46. Acunzo M, Croce CM. MicroRNA in Cancer and Cachexia – A Mini-Review. *J Infect Dis*. 2015;212(Suppl 1):S74–S77.
47. Li WT, Zheng H, Nguyen V, Wang-Rodriguez J, Ongkeko WM. Functional Genomics Profiling of Bladder Urothelial Carcinoma MicroRNAome as a Potential Biomarker. *Neoplasia*. 2018;20(4):364–373.
48. Nagai T, Arao T, Nishio K, et al. Impact of Tight Junction Protein ZO-1 and TWIST Expression on Postoperative Survival of Patients with Hepatocellular Carcinoma. *Dig Dis*. 2016;34(6):702–707.
49. Tang O, Chen XM, Shen S, Hahn M, Pollock CA. MiRNA-200b represses transforming growth factor-β1-induced EMT and fibronectin expression in kidney proximal tubular cells. *Am J Physiol Renal Physiol*. 2013;304(10):F1266–F1273.

Supplementary material

Table S1 Association of miR-30a-5p expression with the HCC clinicopathological characteristics and several parameters

Variable	Relative miR-431-5p expression		χ^2	*P*-value
	Low (%)	High (%)		
N	19 (50)	19 (50)		
Age (years)				
≤45	9 (23.68)	7 (18.42)	0.43	0.51
>45	10 (26.32)	12 (31.58)		
HBsAg				
Negative	12 (31.58)	16 (42.11)	1.22	0.27
Positive	7 (18.42)	3 (7.89)		
AFP (μg/L)				
>20	14 (36.84)	13 (34.21)	0.13	0.72
≤20	5 (13.16)	6 (15.79)		
Tumor size (cm)				
>3	17 (44.74)	10 (26.32)	4.61	0.03
≤3	2 (5.26)	9 (23.68)		
Tumor amount				
1	14 (36.84)	8 (21.05)	3.89	0.05
>1	5 (13.16)	11 (28.95)		
Tumor encapsulation				
Positive	6 (15.79)	15 (39.47)	6.81	0.01
Negative	13 (34.21)	4 (10.53)		
Vascular invasion				
Positive	10 (26.32)	2 (5.26)	5.97	0.01
Negative	9 (23.68)	17 (44.74)		
5-year survival				
Yes	1 (2.63)	8 (21.05)	5.24	0.02
No	18 (47.37)	11 (28.95)		
5-year recurrence				
Yes	19 (50)	15 (39.47)	–	0.11
No	0 (0)	4 (10.53)		
UROC28 level				
Low	2 (5.26)	11 (28.95)	7.48	0.00
High	17 (44.74)	8 (21.05)		

Abbreviations: HBsAg, hepatitis B surface antigen; HCC, hepatocellular carcinoma.